Supplementary Figure 1

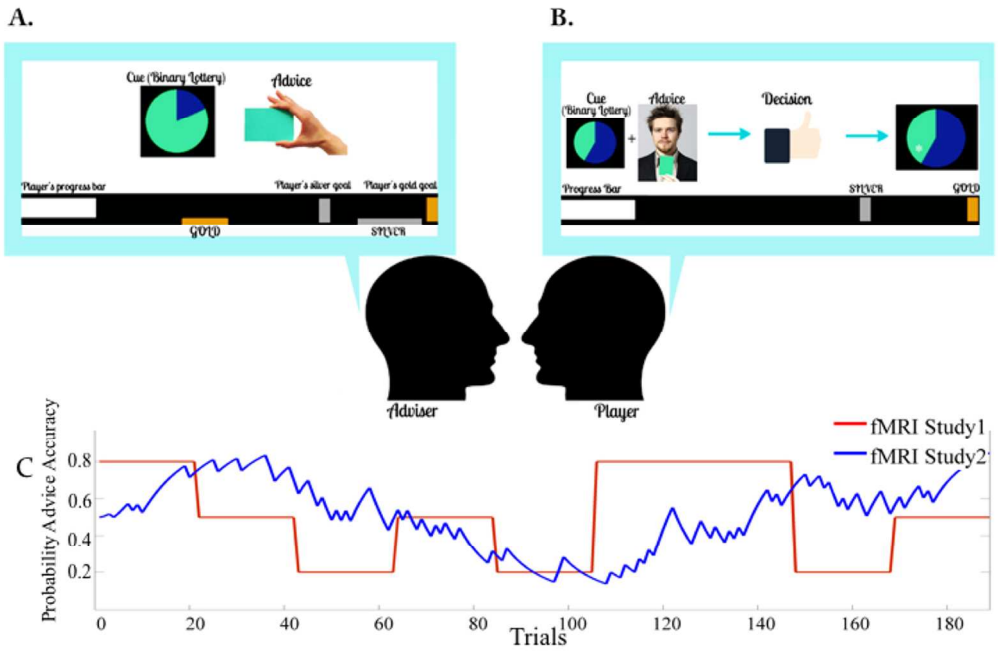

Supplementary Figure 1| Experimental Paradigm: Roles and Incentive Structure: Two sets of participants randomly assigned to adviser (A) and player roles (B) took part in an advice-taking game for monetary rewards, in which they had to predict the outcome of a binary lottery. If they reached the silver target, they received an extra bonus of CHF 10 (Swiss Francs); if they reached gold, they received an extra CHF 20. They benefited from considering the other player's advice. The adviser, whose recommendations were pre-recorded and presented via video, received more information about the outcome (constant probability of 80%), and based on this information, advised the player on which option to choose. Critically, the adviser's motivation to provide valid or misleading information varied during the game as a function of his incentive structure: If the participant's score landed within the adviser's silver range at the end of the game, the adviser received an extra CHF 10; if the score landed in the adviser's golden range, the adviser earned an extra CHF 20. Importantly, before the experiment participants were informed (truthfully) that the adviser had his own undisclosed incentives and thus his intentions could change during the game. (C) While the input structure was based on the dominant strategy of the advisers, the volatility schedule was optimized using simulations in the second fMRI study. The objective function used was minimizing the correlations between the hierarchical PEs.

Supplementary File

529x396mm (72 x 72 DPI)

Supplementary Figure 2

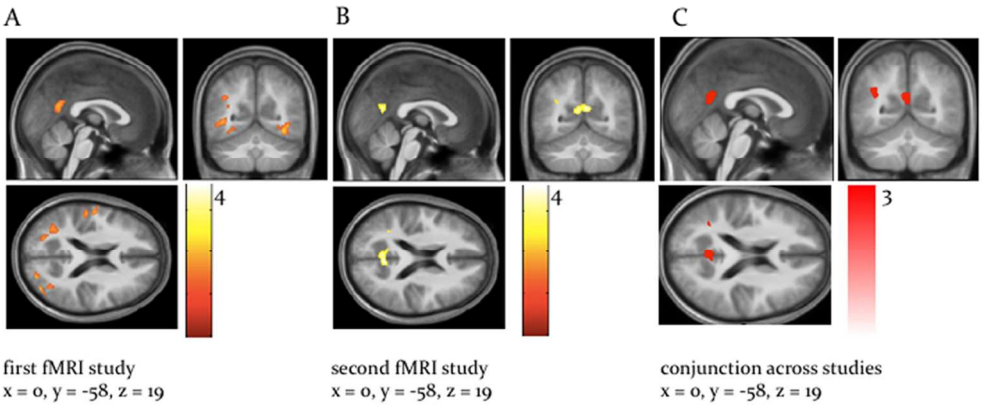

Supplementary Figure 2| Positive correlations with epsilon2: Activations in response to positive signed precision-weighted PE about the adviser fidelity in the first (A) and the second fMRI study (B). Both activation maps are shown at a threshold of $p<0.05$, cluster-level FWE corrected for multiple comparisons across the whole brain. To highlight replication across studies, panel C shows the results of a "logical AND" conjunction, illustrating voxels that were significantly activated in both studies.

Supplementary File

352x195mm (72 x 72 DPI)

Supplementary Figure 3

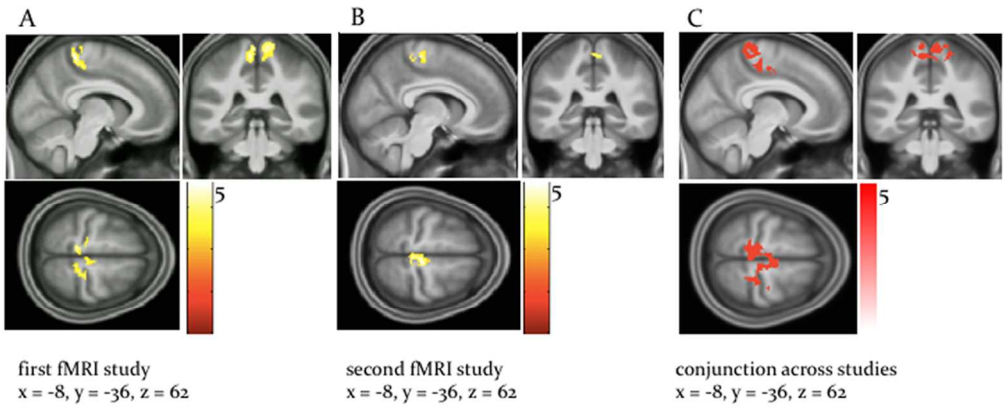

Supplementary Figure 3 | Negative correlations with epsilon3: Activations in response to decreases in signed precision-weighted PE about the adviser's strategy in the first (A) and the second fMRI study (B). Both activation maps are shown at a threshold of $p<0.05$, cluster-level FWE corrected for multiple comparisons across the whole brain. To highlight replication across studies, panel C shows the results of a "logical AND" conjunction, illustrating voxels that were significantly activated in both studies.

Supplementary File

352x183mm (72 x 72 DPI)

Supplementary Figure 4

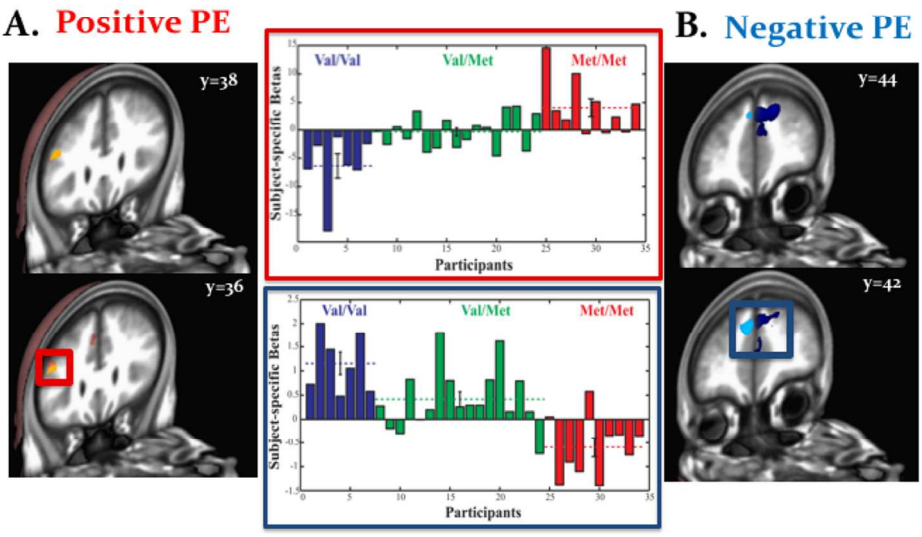

Supplementary Figure 4| Advice PEs and correlations with the COMT SNP: ‼ ┼ (A) Positive precision-weighted PEs (on trials when the advice was more helpful than predicted) were associated with increased activity in the left dorsolateral PFC (t(34) = 5.10, whole-brain FWE correction at the cluster level, $p < 0.05$). Participants with the Met/Met polymorphism (and reduced efficacy of the COMT enzyme) showed a larger representation of positive precision-weighted advice PEs in the left dorsolateral PFC compared to Val/Val allele carriers (upper middle panel; t(34) = 5.82, whole-brain FWE correction at the cluster level, $p < 0.05$). (B) Negative precision-weighted PEs (on trials when the advice was more misleading than predicted) were associated with increased activity in the bilateral dorsomedial PFC and the superior occipital cortex (whole-brain FWE correction at the cluster level, $p < 0.05$). Participants with the Met/Met polymorphism showed reduced activity for negative PEs in the dorsomedial PFC and the fusiform face area (FFA) compared to carriers of the Val allele (lower middle panel; whole-brain FWE correction at the cluster level, $p < 0.05$).
Supplementary File
529x333mm (72 x 72 DPI)

Supplementary Figure 5

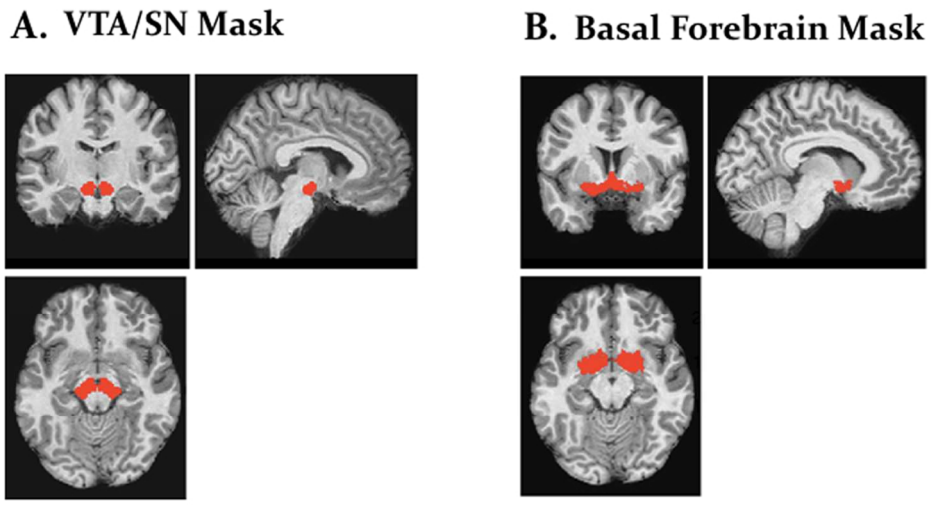

Supplementary Figure 5| Anatomical masks: ‼ ┼ (A) The VTA/SN mask created using an anatomical atlas based on magnetization transfer weighted structural MR images (see Bunzeck and Düzel, 2006). (B) The basal forebrain mask created using the anatomical toolbox in SPM12 (http://www.fil.ion.ucl.ac.uk/spm).‼ ┼
Supplementary File
352x215mm (72 x 72 DPI)

Figures

Supplementary Figures

Supplementary Figure 1| **Experimental Paradigm: Roles and Incentive Structure**

Two sets of participants randomly assigned to adviser (A) and player roles (B) took part in an advice-taking game for monetary rewards, in which they had to predict the outcome of a binary lottery. If they reached the silver target, they received an extra bonus of CHF 10 (Swiss Francs); if they reached gold, they received an extra CHF 20. They benefited from considering the other player's advice. The adviser, whose recommendations were pre-recorded and presented via video, received more information about the outcome (constant probability of 80%), and based on this information, advised the player on which option to choose. Critically, the adviser's motivation to provide valid or misleading information varied during the game as a function of his incentive structure: If the participant's score landed within the adviser's silver range at the end of the game, the adviser received an extra CHF 10; if the score landed in the adviser's golden range, the adviser earned an extra CHF 20. Importantly, before the experiment participants were informed (truthfully) that the adviser had his own undisclosed incentives and thus his intentions could change during the game. (C) While the input structure was based on the dominant strategy of the advisers, the volatility schedule was optimized using simulations in the second fMRI study. The objective function used was minimizing the correlations between the hierarchical PEs.

Supplementary Figure 2| **Positive correlations with ε_2**
Activations in response to positive signed precision-weighted PE about the adviser fidelity in the first (A) and the second fMRI study (B). Both activation maps are shown at a threshold of $p<0.05$, cluster-level FWE corrected for multiple comparisons across the whole brain. To highlight replication across studies, panel C shows the results of a "logical AND" conjunction, illustrating voxels that were significantly activated in both studies.

Supplementary Figure 3 | **Negative correlations with ε_3**
Activations in response to decreases in signed precision-weighted PE about the adviser's strategy in the first (A) and the second fMRI study (B). Both activation maps are shown at a threshold of $p<0.05$, cluster-level FWE corrected for multiple comparisons across the whole brain. To highlight replication across studies, panel C shows the results of a "logical AND" conjunction, illustrating voxels that were significantly activated in both studies.

Supplementary Figure 4| **Advice PEs and correlations with the COMT SNP**:
(A) Positive precision-weighted PEs (on trials when the advice was more helpful than predicted) were associated with increased activity in the left dorsolateral PFC ($t(34) = 5.10$, whole-brain FWE correction at the cluster level, $p < 0.05$). Participants with the Met/Met polymorphism (and reduced efficacy of the COMT enzyme) showed a larger

representation of positive precision-weighted advice PEs in the left dorsolateral PFC compared to Val/Val allele carriers (upper middle panel; $t(34) = 5.82$, whole-brain FWE correction at the cluster level, $p < 0.05$). (B) Negative precision-weighted PEs (on trials when the advice was more misleading than predicted) were associated with increased activity in the bilateral dorsomedial PFC and the superior occipital cortex (whole-brain FWE correction at the cluster level, $p < 0.05$). Participants with the Met/Met polymorphism showed reduced activity for negative PEs in the dorsomedial PFC and the fusiform face area (FFA) compared to carriers of the Val allele (lower middle panel; whole-brain FWE correction at the cluster level, $p < 0.05$).

Supplementary Figure 5| **Anatomical masks**:
(A) The VTA/SN mask created using an anatomical atlas based on magnetization transfer weighted structural MR images (see Bunzeck and Düzel, 2006). (B) The basal forebrain mask created using the anatomical toolbox in SPM12 (http://www.fil.ion.ucl.ac.uk/spm).

Tables

Supplementary Table 1: Prior mean and variance of the perceptual and response model parameters [reprinted from Diaconescu et al., 2014]

Parameter	Prior mean	Prior variance
(i) HGF model class $M_1 \dots M_6$		
κ	0.5	1
ω	-2	100
ϑ	0.5	1
$\mu_2^{(k=0)}$	0	1
$\sigma_2^{(k=0)}$	1	1
$\mu_3^{(k=0)}$	1	1
$\sigma_3^{(k=0)}$	1	1
(ii) No Volatility HGF model class $M_7 \dots M_9$		
κ	0.5	0
ω	-2	100
ϑ	0.5	0
$\mu_2^{(k=0)}$	0	1
$\sigma_2^{(k=0)}$	1	1
$\mu_3^{(k=0)}$	1	0
$\sigma_3^{(k=0)}$	1	0
(iii) Rescorla-Wagner model class $M_{10} \dots M_{12}$		
α	0.2	1
$v^{(k=0)}$	0.5	1
(iv) Integrated model class M_1, M_4, M_7, M_{10}		
ζ	0	1
β	48	1
(v) Reduced: Advice M_2, M_5, M_8, M_{11}		
ζ	∞	0
β	48	1
(vi) Reduced: Cue model class M_3, M_6, M_9, M_{12}		
ζ	$-\infty$	0
β	48	1

Note: The prior variances are given in the space in which parameters are estimated. κ, ϑ, α, $\mu_2^{(k=0)}, \mu_3^{(k=0)}, \boldsymbol{v}^{(k=0)}$ and ζ are estimated in logit-space, while σ_2, σ_3 and β are estimated in log-space.

Supplementary Table 2: Neural Representations of positive, low-level precision-weighted PEs

	Hemisphere	x	y	z	*t score*
fMRI study 1: positive correlations epsilon 2					
TPJ	L	-40	-43	27	3.33
middle temporal cortex	R	40	-54	-3	3.85
fusiform gyrus	L	-28	-72	-8	3.46
fMRI study 2: positive correlations epsilon 2					
precuneus	L	0	-58	19	5.38
conjunction: positive correlations epsilon 2					
precuneus	L	0	-58	19	2.71

Supplementary Table 3: Negative correlations with high-level precision-weighted PEs

	Hemisphere	x	y	z	*t score*
fMRI study 1: epsilon 3 negative correlations					
supplementary motor area	R	12	-22	48	6.85
middle cingulate sulcus	R	9	-13	40	5.48
middle cingulate sulcus	L	-16	-43	37	5.77
fMRI study 2: epsilon 3 negative correlations					
middle cingulate sulcus	L	-8	-36	62	5.21
paracentral lobule	R	8	-24	72	5.19
conjunction: epsilon 3 negative correlations					
middle cingulate sulcus	R	4	-19	52	4.43
paracentral lobule	R	8	-30	57	3.87